

EPiC Series in Computing

Volume 114, 2026, Pages 1–9

Proceedings of the Workshop on Mathematical Modeling and Scientific Computing



A Combined Domain Decomposition and Lagrange Multiplier Method for Multi-Contact Inelastic Thermomechanics

Pavel S. Aronov, Mikhail P. Galanin, and Alexandr S. Rodin

Keldysh Institute of Applied Mathematics RAS, Moscow, Russia
aronovps@mail.ru
galan@keldysh.ru
rals@bk.ru

Abstract

An efficient numerical algorithm is proposed for solving multi-contact thermomechanical problems and applied to simulate a fuel element section. The mathematical model employs an axisymmetric thermoelastic approximation incorporating creep and body contact interaction. The numerical implementation combines the finite element method and the Lagrange multiplier method with mortar mesh discretization. A distinctive feature of the algorithm is the decomposition of the fuel column into overlapping subdomains. Within the iterative process, local contact problems are combined into a global solution using a correction term obtained from an auxiliary problem on a coarse grid. The computational results confirmed a weak dependence of the number of iterations on the number of fuel pellets. This property of the algorithm can potentially be exploited for parallel implementation and simulation of full-scale fuel rods.

1 Introduction

In structural modeling, incorporating component contact interactions drastically drives up computational complexity — especially when dealing with numerous parts and unpredictable contact zones. To address this, the present paper considers algorithms for multi-contact problems with a designated direction, where the contacting components are aligned along a single axis to form a column-like structure. An efficient approach in this context is the domain decomposition method (DDM) [11, 13]: the computational domain is partitioned into subdomains along the designated direction, a local contact problem is solved within each subdomain, and the solutions are subsequently merged into a global one.

A nuclear reactor fuel rod (fuel element) is taken as an illustrative example [7]. Its primary component is a fuel column consisting of hundreds of nuclear fuel pellets. Due to the generated heat, the pellets deform and swell, which can result in cladding failure or issues at the column extremities, potentially leading to an accident. Therefore, numerical modeling of the thermomechanical behavior of the fuel rod under various reactor operating regimes is highly relevant.

V. Turova, A. Kovtanyuk, A. Maslovskaya and J. Zimmer (eds.), MMSC 2026 (EPiC Series in Computing, vol. 114), pp. 1–9

The operating lifecycle of a fuel rod typically spans several years. Over this period, substantial creep strains develop within it, exerting a significant influence on its stress-strain state.

Previously, the authors modeled the contact interaction of pellets using, for instance, a combination of a two-level additive Schwarz method and a Neumann–Dirichlet method [8] (which requires additional iterations when solving local problems) and a mortar method combined with a modified symmetric successive over-relaxation (MSSOR) method [1] (which requires a strictly sequential solution of local linear systems of equations for each pellet).

In [3], a numerical algorithm based on the mortar method was presented and applied to simulate the thermomechanical state of a fuel rod section composed of 10 pellets, taking into account material creep and cracking. In [4], the authors developed a combination of a two-level additive Schwarz method and a mortar method, but its application was limited to the thermoelastic approximation.

The present work extends this framework to incorporate material creep within the two-level parallel domain decomposition method, enabling large-scale, long-term thermomechanical simulations. The specific contribution of this paper lies in scaling the computational capability up to a 50-pellet fuel rod section and demonstrating the algorithm's stability and efficiency over a 1-year operational timeline. Furthermore, a comprehensive convergence and scalability analysis is provided to demonstrate how the robust numerical features of the developed two-level algorithm remain fully preserved when incorporating nonlinear, time-dependent material behavior.

2 Mathematical formulation of the problem

Consider a structure composed of N axisymmetric bodies that occupies the domain $G = \bigcup_{i=1}^{N} G_i$ with the boundary ∂G. The mathematical model of the quasistatic problem in solid mechanics includes the following relations for $t > 0$ [12, 13]:

- equilibrium equations

$$L\mathbf{u}(t) = -\nabla \cdot \boldsymbol{\sigma}(\mathbf{u}, t) = 0, \quad \mathbf{x} \in G, \tag{1}$$

- boundary conditions (kinematic and traction)

$$\mathbf{u}(\mathbf{x}, t) \cdot \mathbf{n} = 0, \quad \mathbf{x} \in \partial G_D, \tag{2}$$

$$\boldsymbol{\sigma}(\mathbf{u}, t) \cdot \mathbf{n} = \mathbf{p}(\mathbf{x}, t), \quad \mathbf{x} \in \partial G_N, \tag{3}$$

- strain-displacement relation for the linear strain tensor

$$\boldsymbol{\varepsilon}(\mathbf{u}) = \frac{1}{2}\left(\nabla \mathbf{u} + (\nabla \mathbf{u})^T\right), \tag{4}$$

- Hooke's law for the stress tensor

$$d\boldsymbol{\sigma}(\mathbf{u}) = \mathbf{C} : \left(d\boldsymbol{\varepsilon}(\mathbf{u}) - d\boldsymbol{\varepsilon}^{th} - d\boldsymbol{\varepsilon}^{c}(\mathbf{x})\right). \tag{5}$$

Here, $\mathbf{u}(\mathbf{x})$ is the displacement vector of a point with the position vector $\mathbf{x} = x_i \mathbf{e}_i$; ∂G_D is the boundary part where the kinematic conditions for the normal component of the displacement vector are prescribed; $\mathbf{p}(\mathbf{x}) = p_i(\mathbf{x})\,\mathbf{e}_i$ is the external load vector acting on the boundary

part ∂G_N; $\mathbf{C}$ is the elasticity tensor; $\boldsymbol{\varepsilon}^{th}$ is the thermal strain tensor; and $\boldsymbol{\varepsilon}^c$ is the creep strain tensor.

It is assumed that different bodies can come into contact with each other; in total, the structure contains Q pairs of potentially contacting surfaces $\left(S^j_{c,1}, S^j_{c,2}\right)$, $j = 1, \ldots, Q$.

To model the creep process, the flow theory of creep [10] is employed, which assumes that the following relation holds for the creep strain rate tensor:

$$\dot{\varepsilon}^c_{ij} = \dot{\mu}\sigma'_{ij}, \tag{6}$$

where $\dot{\mu} = \frac{3}{2}\frac{\dot{\varepsilon}^c_*}{\sigma_*}$, $\sigma_* = \sqrt{\frac{3}{2}\sigma'_{kl}\sigma'_{kl}}$ is the equivalent stress (stress intensity), $\dot{\varepsilon}^c_* = f(T, \sigma_*)$ is the creep strain rate relation, and $\sigma'_{kl} = \sigma_{kl} - \frac{1}{3}\sigma_{mm}\delta_{kl}$.

The frictionless sliding conditions for the surface $S^j_{c,1}$ can be written in the following form (and similarly for the boundary $S^j_{c,2}$) [15]:

$$\sigma_\tau(\mathbf{x}) = 0, \tag{7}$$
$$\sigma_n(\mathbf{x}) = \sigma_n(\bar{\mathbf{x}}) \leqslant 0, \tag{8}$$
$$u_n(\mathbf{x}) + u_n(\bar{\mathbf{x}}) \leqslant \delta_{0n}(\mathbf{x}), \tag{9}$$
$$\sigma_n(\mathbf{x})\left[u_n(\mathbf{x}) + u_n(\bar{\mathbf{x}}) - \delta_{0n}(\mathbf{x})\right] = 0, \tag{10}$$

where $\bar{\mathbf{x}} \in S^j_{c,2}$ is the corresponding (closest) point to $\mathbf{x} \in S^j_{c,1}$; $\delta_{0n}(\mathbf{x}) \geqslant 0$ is the function defining the initial clearance (gap) between the surfaces; $\mathbf{n}$ and $\boldsymbol{\tau}$ are the outward unit normal vector and the tangent vector at the point under consideration, respectively; $u_n = \mathbf{u}\cdot\mathbf{n}$; $\sigma_n = (\boldsymbol{\sigma}\cdot\mathbf{n})\cdot\mathbf{n}$; and $\sigma_\tau = (\boldsymbol{\sigma}\cdot\mathbf{n})\cdot\boldsymbol{\tau}$.

In the following, the vector inequality $\mathbf{g}(\mathbf{x}) \leqslant 0$ will be used to denote the block of boundary conditions (7)–(10).

3 Numerical model

In the general case, the final configuration of the contacting surfaces is not known a priori; therefore, problem (1)–(10) is non-linear. To solve it, we employ a combination of a two-level additive Schwarz method and a mortar method proposed in [4].

The **mortar method** [6,14] is based on an independent finite element discretization of non-overlapping domains, allowing for the use of non-matching grids (meshes) at the interfaces between bodies, whereas solution continuity is enforced using Lagrange multipliers defined on a separate mortar grid.

Applying the Lagrange multiplier method allows reducing the original problem at a time instance t_s to the minimization problem of the following functional [15]:

$$\Pi(t_s) = \frac{1}{2}\int\limits_G \sigma_{ij}\varepsilon_{ij}dG - \int\limits_{\partial G_N} u_i p_i dS + \int\limits_{S^k_c} \lambda_i(\mathbf{x},t)\left(u_i(\mathbf{x},t) + u_i(\bar{\mathbf{x}},t) - \delta_{0i}(\mathbf{x},t)\right)dS, \tag{11}$$

where $\boldsymbol{\lambda} = (\lambda_\tau \quad \lambda_n)^T$ is the Lagrange multiplier (for the frictionless sliding condition, $\lambda_\tau = 0$), and S^k_c is the union of all mortar grids corresponding to different pairs of contact surfaces.

For the spatial discretization of the resulting equations, the finite element method (FEM) [5] is applied. Note that an iterative process is used during the linearization of (11), within which

a known configuration of the contact surfaces taken from the previous iteration is used at the beginning of the iteration, and then its correction is performed at the end of the iteration. A detailed description of the mortar-based algorithm and the specifics of its application to solving multi-contact problems are provided in [1].

After applying the standard FEM procedures, problem (11) at the $(m+1)$-th iteration is reduced to solving the following system of linear equations:

$$\begin{bmatrix} K & M^{(m)} \\ M^{(m)T} & 0 \end{bmatrix} \begin{Bmatrix} \Delta U^{(m+1)} \\ \Delta\lambda^{(m+1)} \end{Bmatrix} = \begin{Bmatrix} R \\ R_\delta \end{Bmatrix}, \tag{12}$$

where $[K]$ is the global stiffness matrix; the matrix $[M]$ arises from the approximation of the integral over all contact surfaces; $\Delta\{U\} = \{U\} - \{\check{U}\}$, where $\{U\}$ and $\{\check{U}\}$ are the global vectors of nodal displacements at the s-th and $(s-1)$-th time steps, respectively; $\{\lambda\}$ is the global vector of Lagrange multipliers; $\{R\}$ is the global vector of nodal forces that accounts for the contribution of surface forces, thermal strains, and creep strains; and $\{R_\delta\}$ is the global vector of nodal forces that accounts for the presence of initial clearances between the contacting surfaces.

The **additive Schwarz method** (a variant of DDM with overlapping subdomains) can also be used to solve the system of equations (1)–(10). Let us represent the domain G as a union $G = \bigcup_{k=1}^{M} \Omega_k$ of a finite number of its subdomains $\Omega_1, \ldots, \Omega_M$ with the boundaries $\partial\Omega_1, \ldots, \partial\Omega_M$ ($\bar{\Omega}_k = \Omega_k \cup \partial\Omega_k$). Within the domain Ω_k, there are n_k mesh nodes.

Let us introduce the notations $\partial\Omega_{N,k} = \partial G_N \cap \partial\Omega_k$, $\partial\Omega_{D,k} = \partial G_D \cap \partial\Omega_k$, and $S_{c,k} = S_c \cap \partial\Omega_k$. At each time instance t_s, we choose a certain function $\mathbf{u}^{(0)}$ that satisfies the boundary condition (2). We then construct a sequence of functions $\{\mathbf{u}^{(m)}\}$. At the $(m+1)$-th iteration, we first solve local contact problems with fixed contact zones (taken from the previous iteration) within the subdomains Ω_k $(k = 1, \ldots, M)$:

$$L\mathbf{u}_k^{(m+1)}(t_s) = \mathbf{0}, \quad \mathbf{x} \in \Omega_k, \tag{13}$$

$$\boldsymbol{\sigma} \cdot \mathbf{n} = \mathbf{p}(\mathbf{x}, t), \quad \mathbf{x} \in \partial\Omega_{N,k}, \tag{14}$$

$$\mathbf{g}(\mathbf{x}, t) \leqslant 0, \quad \mathbf{x} \in S_{c,k}, \tag{15}$$

$$\mathbf{u}_k^{(m+1)}(\mathbf{x}, t) = \mathbf{u}^{(m)}(\mathbf{x}, t), \quad \mathbf{x} \in \bar{G} \backslash (\Omega_k \cup \partial\Omega_{N,k} \cup S_{c,k}). \tag{16}$$

At the end of each iteration, the final solution is calculated using the formula

$$\mathbf{u}^{(m+1)}(t_s) = \mathbf{u}^{(m)}(t_s) + \alpha \sum_{k=1}^{M} \mathbf{w}_k^{(m+1)}(t_s), \tag{17}$$

where

$$\mathbf{w}_k^{(m+1)}(t_s) = \mathbf{u}_k^{(m+1)}(t_s) - \mathbf{u}^{(m)}(t_s). \tag{18}$$

In the constructed algorithm, the modification of the contact surfaces is not taken into account when solving the local problems (13)–(16); instead, it is performed simultaneously across the entire domain at the end of the outer iteration. The update of the creep strain vector is also carried out during the outer iteration.

Note that the solution of the local problems (13)–(16) in different subdomains can be performed independently of each other; therefore, such an algorithm can be quite easily parallelized in the future.

As shown in [13] (for linear problems), as the number of introduced subdomains increases, the number of outer iterations required to achieve a specified accuracy level in the additive Schwarz method can multiply. Such a dependence significantly impairs the efficiency of the method. To overcome this drawback, an additive Schwarz method with coarse-grid correction is employed, which assumes that along with the fine computational mesh, a coarse mesh is defined in the domain, with cell sizes comparable to the sizes of the introduced subdomains. The nodes of the coarse mesh do not necessarily coincide with those of the fine mesh, and the boundaries of the coarse computational domain may differ from the boundaries of the original computational domain. Hereinafter, such a method will be referred to as a two-level method, whereas the method without coarse-grid correction will be called a one-level method.

In the two-level additive Schwarz method, the global displacement vector is calculated by the formula [13]:

$$\left\{U^{(m+1)}\right\} = \left\{U^{(m)}\right\} + \alpha \sum_{k=0}^{M} \left\{w_k^{(m+1)}\right\}, \tag{19}$$

where the correction vector $w_0^{(m+1)}$ for the solution on the fine mesh is computed using the residual vector of the auxiliary problem solved on the coarse mesh without considering contact [4].

After applying the FEM for spatial discretization, the local problem k from (13)–(16) reduces to a system of equations analogous to (12).

A more detailed description of the algorithm based on the two-level additive Schwarz method applied to multi-contact problems is provided in [1]. The numerical algorithm for modeling creep deformation with an automatic time-step selection is detailed in [2].

4 Numerical results

In the computations, second-order finite elements on a quadrilateral mesh [5] are used to interpolate displacements and Lagrange multipliers, and the following input parameters are prescribed: $\left\{U^{(0)}\right\} = 0$ at the first time step, $\left\{U^{(0)}\right\} = \left\{\check{U}\right\} = 0$ at the remaining steps, $\alpha = 0.25$, and $\varepsilon_0 = 10^{-6}$, where ε_0 is the specified tolerance defining when the iterative process terminates. Specifically, this tolerance is applied to the relative difference between the displacement vectors at consecutive iterations, computed in the L_2 norm [4].

The problem of the contact interaction between uranium dioxide pellets in a fuel column, which is the most critical part of a nuclear fuel rod (fuel element), is solved [1, 8]. Simulation of a fuel rod section comprising up to 50 fuel pellets is performed over a time interval of up to one year (the typical operating lifetime of a fuel rod is several years). A pellet is a cylinder with a central hole and chamfers on both ends. The fuel column usually includes several hundred pellets and is located inside a cylindrical zirconium alloy cladding. During the fuel rod operation, the pellets are heated to a temperature of approximately 1600 K and come into contact with each other. As a rule, an initial gap exists between the cladding and the fuel column. For certain fuel rod operating regimes, the pellets come into contact with the cladding due to thermal and radiation-induced swelling, but no such contact occurs in the present work.

The computational domain included $\tilde{N}$ pellets and a section of the cladding (a total of $N = \tilde{N} + 1$ bodies). At the first stage, a dynamic thermal problem was solved with a prescribed constant (in space) heat generation density in the pellets; a heat transfer boundary condition with the cladding was specified on the lateral surfaces of the pellets, and the cladding temperature was assumed to be constant (623 K).

After the temperature reached a steady-state regime (at the time instance of 1 hour), a mechanical problem was solved at the second stage using the obtained temperature field

and the following boundary conditions: the bottom ends of the first pellet and the cladding are fixed along the Oz axis, a pressure of $p_1 = 10$ MPa is prescribed on the top end of the upper pellet, and a pressure of $p_2 = 10$ MPa is prescribed on the outer surface of the cladding. A frictionless sliding condition is specified on the surfaces of the contacting bodies. To account for realistic material properties (zirconium alloy for the cladding and uranium dioxide for the fuel pellets), procedures from the MATPRO library [9] are utilized.

In the additive Schwarz method, the computational domain is partitioned into non-overlapping subdomains $\bar{\Omega}_1, \ldots, \bar{\Omega}_M$, $M = N+1$. Subdomain $\bar{\Omega}_1$ is the union of the bottom half of the lowermost pellet and its corresponding cladding section; $\bar{\Omega}_M$ is the union of the top half of the uppermost pellet and its corresponding cladding section; for other cases ($k = 2, \ldots, M-1$), $\bar{\Omega}_k$ is the union of the top half of the k-th pellet, the bottom half of the $(k+1)$-th pellet, and their corresponding cladding section. The overlapping subdomain Ω_k is obtained by combining the subdomain $\bar{\Omega}_k$ with additional segments of the neighboring subdomains $\bar{\Omega}_{k-1}$ and $\bar{\Omega}_{k+1}$, whose dimensions are determined by the chosen relative overlap coefficient (typically 0.3). The coarse mesh was constructed for two bodies: the first body corresponded to the union of all pellets without considering their chamfers, and the second body coincided with the cladding. In the radial direction, one cell was placed; in the axial direction, the cell size was chosen to be equal to half the pellet height.

In the computations, the following meshes were used (per single pellet): mesh 1 consisted of 10 cells in the radial direction and 20 cells in the axial direction; mesh 2 consisted of 20 cells in the radial direction and 40 cells in the axial direction; mesh 3 consisted of 40 cells in the radial direction and 80 cells in the axial direction. The mesh sizes in the cladding are comparable to the mesh sizes in the pellet.

In all computations, the configuration of the contact surfaces was adjusted. As a result, a non-linear problem was solved, for the linearization of which an additional iterative process was conducted. The correction of the contact surfaces was performed at the end of each iteration; the process converged when the configuration of the contact surfaces stabilized.

Table 1 presents the number of time steps and the total number of outer iterations for the combination of the mortar method and the two-level DDM. Mesh 1, mesh 2, and mesh 3 were used as the fine computational meshes.

Table 1: Number of time steps and outer iterations for different numbers of pellets $\tilde{N}$.

Grid / Parameter	$\tilde{\mathbf{N}} = \mathbf{2}$	$\tilde{\mathbf{N}} = \mathbf{5}$	$\tilde{\mathbf{N}} = \mathbf{10}$	$\tilde{\mathbf{N}} = \mathbf{25}$	$\tilde{\mathbf{N}} = \mathbf{50}$
Mesh 1: Time steps	7	9	13	20	35
Mesh 1: Outer iterations	1573	2031	2960	4556	7975
Mesh 2: Time steps	17	21	28	41	65
Mesh 2: Outer iterations	3840	4762	6410	9384	14881
Mesh 3: Time steps	32	39	49	68	85
Mesh 3: Outer iterations	7259	8850	11215	15562	19443

Figure 1 shows the plots of the number of iterations and the solution time for the system of linear equations (in seconds) throughout the entire computation (1 year $\approx 3.15 \cdot 10^7$ s) for mesh 2. As seen from Fig. 1(a), at the initial stage (where the contact surface configuration changes significantly), the number of iterations substantially exceeds its level during the time

interval when the position of the contact surfaces has established and remains unchanged (most of the adjacent pellet ends have come out of contact, with only a few mesh elements near the central holes remaining in contact). Furthermore, as the number of pellets increases, the average number of iterations per time step remains virtually constant ($O(1)$). Fig. 1(b) demonstrates that with an increasing number of pellets, the total time spent solving the systems of linear equations grows according to a near-linear dependence ($O(\tilde{N})$).

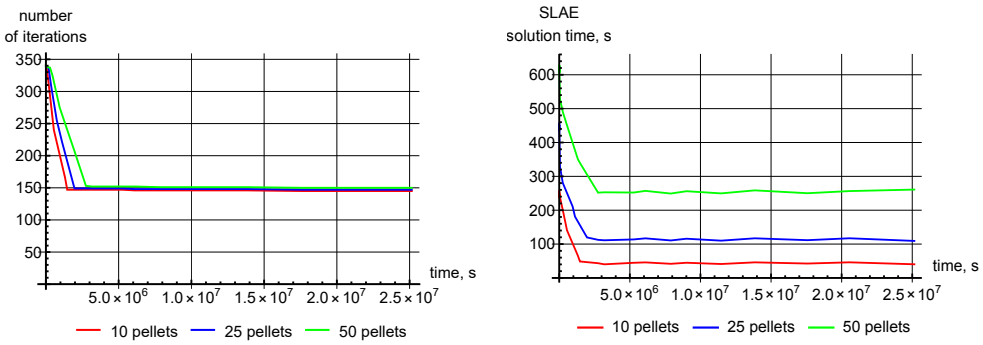

(a) (b)

Figure 1: (a) evolution of the outer iterations count per time step;
(b) corresponding solution time for the linear systems of equations at each time step

As shown in [4], when solving mechanical contact problems where the position of the contact surfaces is not known a priori and can change substantially during loading, the considered combined algorithm of the mortar method and the two-level DDM is more efficient for a sufficiently large number of bodies (greater than 10) compared to the standard mortar method.

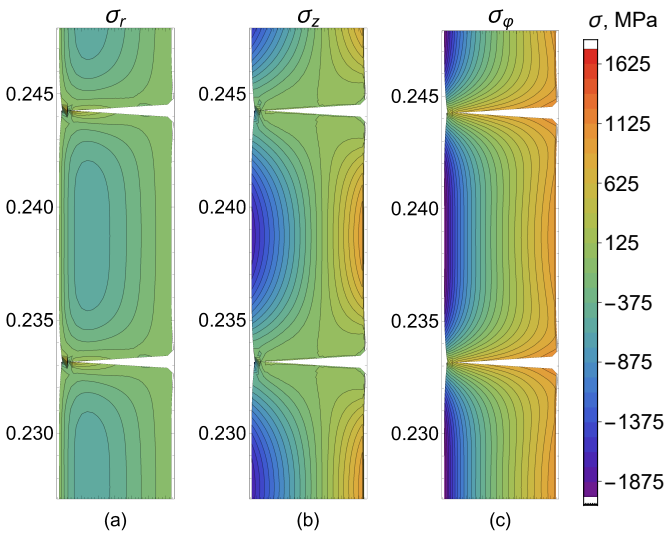

Figure 2: (a) radial stresses (1 hour), (b) axial stresses (1 hour);
(c) circumferential stresses (1 hour)

Figures 2–3 show the two-dimensional distributions of radial, axial, and circumferential stresses (in MPa) for the computation with 50 pellets at the time instances of 1 hour (Fig. 2) and 1 year (Fig. 3). Fragments of the distributions corresponding to the top part of the 23rd pellet, the entire 24th pellet, and the bottom part of the 25th pellet are presented, where the displacements applied during the reconstruction of the deformed bodies are magnified by a factor of 10 for better clarity. As can be seen from the figures, due to the effect of creep, the values of all stress components within the pellets decrease by a factor of 4–5 over the 1-year time interval.

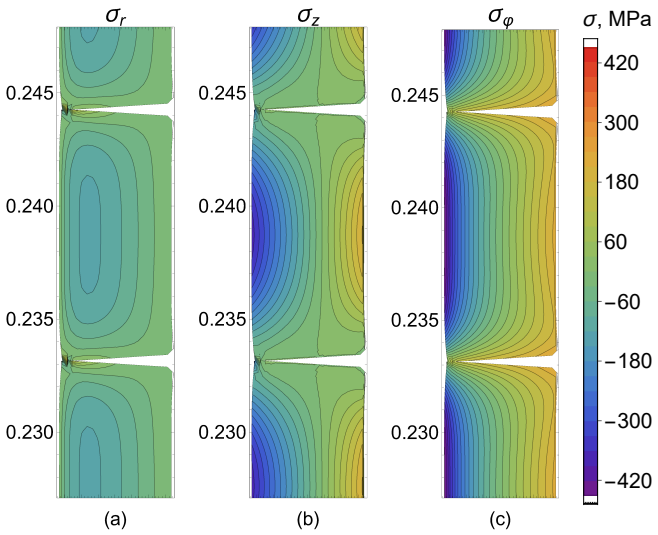

Figure 3: (a) radial stresses (1 year), (b) axial stresses (1 year); (c) circumferential stresses (1 year)

5 Conclusion

The problem of the contact interaction within a system of thermoelastic bodies forming a column-like structure has been solved. To this end, a computational algorithm has been developed that combines the mortar method (a variant of the Lagrange multiplier method) and the two-level additive Schwarz method (a variant of the domain decomposition method with overlapping subdomains). Within this framework, the computational domain is partitioned along a designated direction into a series of subdomains, in each of which a local contact problem is solved autonomously. The obtained results are merged into a global solution that converges to the original one through an iterative process. To accelerate convergence, an additional term obtained from an auxiliary problem solved on a coarse mesh is incorporated into the global solution.

The efficiency of the algorithm has been demonstrated through the simulation of the contact interaction between fuel pellets in a fuel rod section under the axisymmetric thermoelastic approximation, incorporating creep effects. The number of pellets in the computational domain varied from 2 to 50, and frictionless sliding conditions were prescribed at the contact interfaces. Changes in the contact surface configuration were accounted for during the solution process. In the numerical modeling of the creep strain evolution, an automatic time-step selection

algorithm was utilized. Analysis of the results revealed that the number of outer iterations required to achieve a specified tolerance remains virtually unchanged both with an increasing number of pellets and upon fine mesh refinement. Concurrently, the total time spent solving the systems of linear equations within a single computation exhibits a linear growth.

References

[1] P. S. Aronov, M. P. Galanin, and A. S. Rodin. Numerical solution of the problem of nuclear fuel element components contact interaction using the mortar method and the domain decomposition method. *Herald of the Bauman Moscow State Technical University, Series Natural Sciences*, 3(96):4–22, 2021. (In Russian).

[2] P. S. Aronov, M. P. Galanin, and A. S. Rodin. Mathematical modeling of the contact interaction of the fuel element section, including up to 100 pellets, taking into account creep. *WSEAS Transactions on Applied and Theoretical Mechanics*, 17:71–78, 2022.

[3] P. S. Aronov, M. P. Galanin, and A. S. Rodin. Development of numerical algorithms for multi-contact problems of mechanics considering various inelastic effects. In *EPiC Series in Computing*, volume 104, pages 25–35. EasyChair, 2024.

[4] P. S. Aronov, M. P. Galanin, and A. S. Rodin. Combination of domain decomposition method and Lagrange multipliers method for solving multi-contact thermomechanical problems. *Differential Equations*, 62(7):868–881, 2026. (In Russian).

[5] K.-J. Bathe. *Finite Element Procedures*. Prentice Hall, Englewood Cliffs, 1996.

[6] F. Ben Belgacem, P. Hild, and P. Laborde. The mortar finite element method for contact problems. *Mathematical and Computer Modelling*, 28(4):263–271, 1998.

[7] B. R. T. Frost. *Nuclear Fuel Elements: Design, Fabrication and Performance*. Pergamon Press, Oxford, 1982.

[8] M. P. Galanin and A. S. Rodin. Investigation and application of the domain decomposition method for modeling a fuel element. *Computational Mathematics and Mathematical Physics*, 62(4):641–657, 2022.

[9] D. L. Hagrman and G. A. Reymann. MATPRO-Version 11: A handbook of materials properties for use in the analysis of light water reactor fuel rod behavior. Technical Report NUREG/CR-0497, TREE-1280, Idaho National Engineering Laboratory, 1979.

[10] N. N. Malinin. *Applied Theory of Plasticity and Creep*. Mashinostroenie, Moscow, 2nd edition, 1975. (In Russian).

[11] G. I. Marchuk. *Methods of Numerical Mathematics*. Springer-Verlag, New York, 2nd edition, 1982.

[12] S. P. Timoshenko and J. N. Goodier. *Theory of Elasticity*. McGraw-Hill, New York, 3rd edition, 1970.

[13] A. Toselli and O. Widlund. *Domain Decomposition Methods: Algorithms and Theory*. Springer, Berlin-Heidelberg, 2005.

[14] B. I. Wohlmuth. A mortar finite element method using dual spaces for the Lagrange multiplier. *SIAM Journal on Numerical Analysis*, 38(3):989–1012, 2000.

[15] P. Wriggers. *Computational Contact Mechanics*. Springer, Berlin-Heidelberg, 2nd edition, 2006.